CRREL Report 79-30

Suppression of river ice by thermal effluents

George D. Ashton

December 1979

Prepared for
DIRECTORATE OF CIVIL WORKS
OFFICE, CHIEF OF ENGINEERS
By
UNITED STATES ARMY
CORPS OF ENGINEERS
COLD REGIONS RESEARCH AND ENGINEERING LABORATORY
HANOVER, NEW HAMPSHIRE, U.S.A.

Unclassified

SECURITY CLASSIFICATION OF THIS PAGE *(When Data Entered)*

REPORT DOCUMENTATION PAGE

READ INSTRUCTIONS BEFORE COMPLETING FORM

1. REPORT NUMBER: CRREL Report 79-30	2. GOVT ACCESSION NO.
3. RECIPIENT'S CATALOG NUMBER	
4. TITLE *(and Subtitle)*: SUPPRESSION OF RIVER ICE BY THERMAL EFFLUENTS	5. TYPE OF REPORT & PERIOD COVERED
	6. PERFORMING ORG. REPORT NUMBER
7. AUTHOR(s): George D. Ashton	8. CONTRACT OR GRANT NUMBER(s)
9. PERFORMING ORGANIZATION NAME AND ADDRESS: U.S. Army Cold Regions Research and Engineering Laboratory, Hanover, New Hampshire 03755	10. PROGRAM ELEMENT, PROJECT, TASK AREA & WORK UNIT NUMBERS: CWIS 31361, CWIS 31362
11. CONTROLLING OFFICE NAME AND ADDRESS: Directorate of Civil Works, Office, Chief of Engineers, Washington, D.C. 20314	12. REPORT DATE: December 1979
	13. NUMBER OF PAGES: 26
14. MONITORING AGENCY NAME & ADDRESS *(if different from Controlling Office)*	15. SECURITY CLASS. *(of this report)*: Unclassified
	15a. DECLASSIFICATION/DOWNGRADING SCHEDULE

16. DISTRIBUTION STATEMENT *(of this Report)*

Approved for public release; distribution unlimited.

17. DISTRIBUTION STATEMENT *(of the abstract entered in Block 20, if different from Report)*

18. SUPPLEMENTARY NOTES

19. KEY WORDS *(Continue on reverse side if necessary and identify by block number)*

Cold regions
Heat transfer
Ice
Ice openings
Rivers
Thermal diffusion
Thermal pollution

20. ABSTRACT *(Continue on reverse side if necessary and identify by block number)*

The ice suppression resulting from discharge of warm water into rivers during winter is analyzed with emphasis on two different cases. In Part I the case of a thermal effluent fully mixed across the flow section is analyzed to include the effects of unsteadiness in the effluent temperature and the meteorological variations. The location of the ice edge is determined either by a 0°C water temperature criterion or an equilibrium ice melting analysis. The choice of the applicable criterion emerges naturally from the analysis even though the location of the ice edge may be considerably different when a steady-state analysis is done. In Part II the case of a side discharge of heated effluent is analyzed, also in an unsteady manner, and the effects of transverse dispersion are included in the analysis. Comparisons are made in both Parts I and II to limited field data that are available.

DD FORM 1 JAN 73 1473 EDITION OF 1 NOV 65 IS OBSOLETE

Unclassified

SECURITY CLASSIFICATION OF THIS PAGE *(When Data Entered)*

PREFACE

This report was prepared by Dr. George D. Ashton, Chief, Snow and Ice Branch, Research Division, U.S. Army Cold Regions Research and Engineering Laboratory. The study was supported by the Office, Chief of Engineers, Directorate of Civil Works, under Work Units 31362, *Theoretical Study of Ice Suppression Possibilities*, and 31361, *Thermal Regimes Disturbed by Man*.

This work was performed while the author was visiting the Hydraulics Laboratory of the Swedish State Power Board in Alvkarleby, Sweden. The use of their computer facilities is appreciated. The report was technically reviewed by D. Calkins and D. Haynes of CRREL.

CONTENTS

ILLUSTRATIONS

Part I

Figure

Part II

Figure

SUPPRESSION OF RIVER ICE BY THERMAL EFFLUENTS

George D. Ashton

PART I. UNSTEADY SUPPRESSION OF RIVER ICE BY FULLY MIXED THERMAL EFFLUENTS

Introduction

Imposition of a dam and a reservoir on a river generally results in the release of water during winter periods at a temperature above that which would ordinarily be experienced without the reservoir. As a result, the ice cover is suppressed in the reach downstream of the dam. The present analysis examines this ice suppression in an unsteady sense by including both the effects of unsteady variation of the meteorological variables and the storage and release of the energy associated with the melting and freezing of the ice cover. The effluent from the reservoir is assumed to be fully mixed over the initial cross section. In Part II of this report, the effects of a side discharge of thermal effluent will be considered so as to include the effects of lateral mixing.

Previous analytical work on the problem is sparse. Dingman et al. (1968) analyzed the steady-state case, that is, assumed constant meteorological conditions and chose as the criterion for the location of the ice edge downstream the point where the water temperature was 0°C. They well recognized the limitations of their steady-state model (Weeks and Dingman 1972). Paily et al. (1974) considered a similar problem but with a step increase in the effluent temperature and inclusion of the effect of longitudinal dispersion. Their criterion for ice edge location was also the location of the 0°C isotherm for open surface conditions. Examination of their results also shows that inclusion of the longitudinal dispersion term has small effect compared with simple nondispersive routing.

In contrast to these analytical studies Donchenko (1978) pointed out that the ice edge responded strongly to changes in the meteorological variables and varying discharges, in one case fluctuating over a range of 80 km. Donchenko also pointed out the necessity of considering the hydrodynamic stability of the leading edge in locating the position of the ice front.

Governing equations

For a flow with temperature uniformly mixed over the depth, with no transverse velocity variations, and steady flow, the governing partial differential equation is

$$\frac{\partial}{\partial t}(D\rho C_p T_w)+\frac{\partial}{\partial x}(DU\rho C_p T_w)=\frac{\partial}{\partial x}\left(DE_x\frac{\partial(\rho C_p T_w)}{\partial x}\right)+\frac{\partial}{\partial z}\left(DE_z\frac{\partial(\rho C_p T_w)}{\partial z}\right)-\phi \tag{1}$$

where D is the depth of flow, T_w is the water temperature, U is the mean velocity in the x (longitudinal) direction, ρ is the density, C_p is the specific heat capacity, z is the transverse coordinate, and E_x and E_z are respectively the longitudinal and transverse mixing coefficients. ϕ is the heat flux at the top surface and there is assumed to be no flux at the bottom. If we assume D, U, ρ and C_p are constant, then the equation may be written in the form

$$\frac{\partial T_w}{\partial t}+U\frac{\partial T_w}{\partial x}=\frac{\partial}{\partial x}\left(E_x\frac{\partial T_w}{\partial x}\right)+\frac{\partial}{\partial z}\left(E_z\frac{\partial T_w}{\partial z}\right)-\frac{\phi}{\rho C_p D}. \tag{2}$$

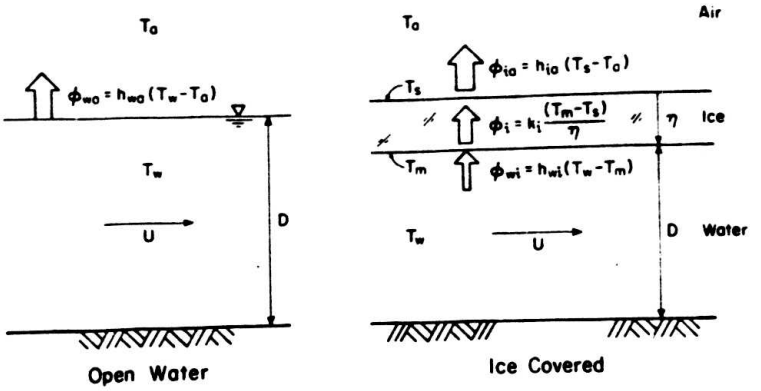

Figure 1. Definition sketch for heat transfer analysis.

We now neglect longitudinal mixing and obtain

$$\frac{\partial T_w}{\partial t} + U\frac{\partial T_w}{\partial x} = \frac{\partial}{\partial z}\left(E_z \frac{\partial T_w}{\partial z}\right) - \frac{\phi}{\rho C_p D}. \quad (3)$$

If we further assume that T_w is fully mixed across the width, then

$$\frac{\partial T_w}{\partial t} + U\frac{\partial T_w}{\partial x} = -\frac{\phi}{\rho C_p D}. \quad (4)$$

Finally, if a Lagrangian viewpoint is adopted we may write

$$\frac{DT_w}{Dt} = -\frac{\phi}{\rho C_p D}. \quad (5)$$

Outline of analysis

A definition sketch is presented in Figure 1.

When the top surface of the flow is open to the atmosphere, $\phi = \phi_{wa}$ where ϕ_{wa} is the heat flux from the water surface to the atmosphere above ϕ_{wa} is a complicated function which has a number of components depending upon air temperature, wind velocity, humidity, cloud cover, time of day and other factors. For present purposes, we will assume the wind speed V_w and air temperature T_a are dominating and express ϕ_{wa} by the simple relationship

$$\phi_{wa} = h_{wa}(T_w - T_a) \quad (6)$$

where h_{wa} is a heat transfer coefficient that is a function of the factors noted above. As a practical matter we will use, in the numerical simulation which follows, a relationship of the form

$$h_{wa} = a + bV_w \quad (7)$$

where a has dimensions of W $m^{-2}°C^{-1}$ and b has dimensions of W $m^{-3}s°C^{-1}$. Depending upon the availability of input data, one may always calculate an equivalent value of a, b or h_{wa} by energy budget analyses. In general, a, b and h_{wa} are functions of time only, since the lengths over which the analysis is carried out are generally much shorter than corresponding spatial variations of the energy budget variables. However, our main purpose here is not to examine refinements in energy budget calculations but rather to examine the implications of the neglect of the unsteadiness of the total flux ϕ and the energy required to melt (or freeze) an ice cover.

When the flow is ice-covered, $\phi = \phi_{wi}$, but now the heat flux from the water to the ice depends upon the flow variables. In particular, we take the heat flux from the water to the ice, ϕ_{wi}, as

$$\phi_{wi} = h_{wi}(T_w - T_m) \quad (8)$$

where h_{wi} is a heat transfer coefficient and T_m is the melting point ($T_m = 0°C$). Closed conduit turbulent heat transfer correlations are generally of the form

$$\frac{h_{wi}R}{k_w} = C\left(\frac{U_w R \rho_w}{\mu}\right)^{0.8}\left(\frac{\mu C_p}{k_w}\right)^{0.4} \quad (9)$$

where R is the hydraulic radius (m), U_w is the average flow velocity (m s^{-1}), ρ_w is the water density (kg m^{-3}), μ is the dynamic viscosity (kg m^{-1} s^{-1}), C_p is the specific heat (J kg^{-1} $°C^{-1}$), and k_w is the thermal conductivity of the water (W m^{-1} $°C^{-1}$). C is an empirical coefficient on the order of 0.023 (see, e.g., Rohsenow and Choi 1961) for smooth surfaces. When the water is above

freezing and the flow is turbulent, relief features (ice ripples) form on the underside of the ice cover which increase the value of C by up to 50% (Ashton and Kennedy 1972). Evaluating the properties at 0°C and taking $R = D/2$,

$$h_{wi} = C_{wi} \frac{U^{0.8}}{D^{0.2}} \tag{10}$$

where $C_{wi} = 1622$ W $s^{0.8}$ $m^{-2.6}$ $°C^{-1}$ for $C = 0.023$ and $C_{wi} = 2433$ W $s^{0.8}$ $m^{-2.6}$ $°C^{-1}$ for $C = 0.0345$.

Equation 5 may now be integrated to yield, in coordinates moving with the flow,

$$\frac{T_w - T_a}{T_{w,0} - T_a} = \exp\left[\frac{-h_{wa}\,(t-t_0)}{\rho C_p D}\right] \text{ open surface} \tag{11}$$

$$\frac{T_w - T_m}{T_{w,0} - T_m} = \exp\left[\frac{-h_{wi}\,(t-t_0)}{\rho C_p D}\right] \text{ ice covered} \tag{12}$$

where the initial condition is taken as $T_w = T_{w,0}$ at $t = t_0$ and $x = x_0$. Relative to coordinates fixed in space such that $dx = Udt$ the corresponding equations are

$$\frac{T_w - T_a}{T_{w,0} - T_a} = \exp\left[\frac{-h_{wa}\,(x-x_0)}{\rho C_p U D}\right] \text{ open surface} \tag{13}$$

$$\frac{T_w - T_m}{T_{w,0} - T_m} = \exp\left[\frac{-h_{wi}\,(x-x_0)}{\rho C_p U D}\right] \text{ ice covered.} \tag{14}$$

Equation 14 is shown in Figure 2 for typical parameter values.

The melting and thickening of the ice cover is governed by the energy balance at the water/ice interface

$$\phi_i - \phi_{wi} = \rho_i \lambda \frac{d\eta}{dt} \tag{15}$$

where ϕ_i is the heat flux by conduction through the ice cover (W m^{-2}), ρ_i is the density of ice (kg m^{-3}), λ is the heat of fusion (J kg^{-1}), η is the ice thickness (m), and $d\eta/dt$ is the rate of thickening. The conductive flux ϕ_i through the ice cover is treated in a quasi-steady manner by assuming a linear temperature profile through the ice thickness. Thus,

$$\phi_i = \frac{k_i\,(T_m - T_s)}{\eta} \tag{16}$$

where k_i is the thermal conductivity of the ice (W m^{-1} $°C^{-1}$), T_s is the top surface temperature of the ice cover, and we require that $T_s \leq 0°C$ because of the state relationship. In the absence of evaporation or condensation on the top surface, $\phi_i = \phi_{ia}$ where ϕ_{ia} is the heat flux from the surface to the atmosphere. ϕ_{ia} may be calculated in a manner similar to ϕ_{wa} through introduction of a heat transfer coefficient h_{ia} applied to the difference $T_s - T_a$ in the form

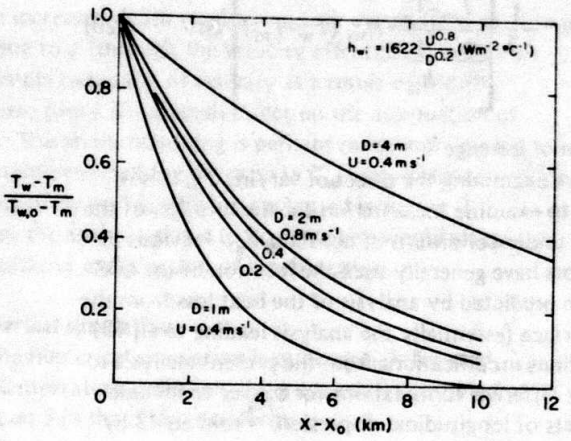

Figure 2. Downstream attenuation of water temperature beneath an ice cover.

$$\phi_{ia} = h_{ia}\,(T_s - T_a). \tag{17}$$

Using $\phi_i = \phi_{ia}$ allows us to eliminate T_s between eq 16 and 17 and results in

$$\phi_i = \frac{T_m - T_a}{\frac{\eta}{k_i} + \frac{1}{h_{ia}}}. \tag{18}$$

We could also in a similar manner add the effects of a snow cover by introducing an additional term η_s/k_s in the denominator of eq 18.

Substitution of eq 18 in eq 15 then results in

$$\frac{T_m - T_a}{\frac{\eta}{k_i} + \frac{1}{h_{ia}}} - h_{wi}(T_w - T_m) = \rho_i \lambda \frac{d\eta}{dt} \tag{19}$$

which, if T_a and T_w are constant in time, may be readily integrated. They seldom are, however, so in the numerical analysis eq 19 will be integrated numerically in stepwise fashion in the form

$$\Delta\eta = \frac{1}{\rho_i \lambda}\left[\frac{T_m - T_a}{\frac{\eta}{k_i}+\frac{1}{h_{ia}}} - h_{wi}\,(T_w - T_m)\right]\Delta t. \qquad (20)$$

Location of ice edge

Before examining the effect of varying T_a, it is of interest to examine the criterion for the location of the ice edge under conditions of constant T_a. Previous investigators have generally used the location of the 0°C isotherm predicted by analysis of the heat loss from the open surface (essentially the analysis leading to eq 13) with various modifications from the present analysis to consider different formulations for ϕ_{wa} or to include the effects of longitudinal dispersion. From eq 13 by the present analysis,

$$(x-x_0)\Big|_{T_w = 0°C} = \frac{-\rho C_p U D}{h_{wa}}\left[\log_e\left(\frac{-T_a}{T_{w,0}-T_a}\right)\right] \qquad (21)$$

Since the heat balance at the surface determines whether or not ice will form at that surface, it is a better indication of the location of the ice edge than is the location of the 0°C isotherm. The condition is obtained by assuming incipient ice formation corresponds to $d\eta/dt = 0$ when $\eta = 0$. From eq 19 this is at a temperature $T_{w,e}$ given by

$$(T_{w,e} - T_m) = \frac{h_{ia}}{h_{wi}}(T_m - T_a). \qquad (22)$$

Substituting into eq 13 the corresponding location is given by

$$(x-x_0)\Big|_{T_{w,e}} = \frac{-\rho C_p U D}{h_{wa}}$$

$$\log_e\left[\frac{T_m - T_a}{T_{w,0}-T_a}\left(1+\frac{h_{ia}}{h_{wi}}\right)\right] \qquad (23)$$

It is now necessary to assume that $h_{ia} = h_{wa}$, which is reasonable at the ice edge since the top surface of the ice edge may be considered wet. The ratio of the distances by the two criteria is then given by

$$\frac{(x-x_0)\Big|_{T_{w,e}}}{(x-x_0)\Big|_{T_w = 0}} = \frac{\log_e\left[\frac{T_m - T_a}{T_{w,0}-T_a}\left(1+\frac{h_{wa}}{h_{wi}}\right)\right]}{\log_e\left[\frac{T_m - T_a}{T_{w,0}-T_a}\right]} \qquad (24)$$

and, of course, the ratio is always less than unity for

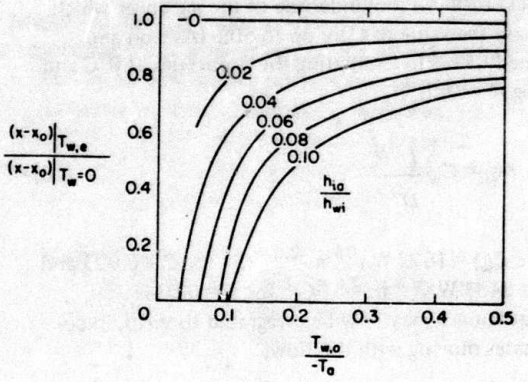

Figure 3. Comparison of distances downstream to edge of ice cover for the criteria of equilibrium heat fluxes and 0°C isotherm location, as a function of the water temperature/air temperature ratio.

$T_a < 0°C$. The ratio is presented in Figure 3 as a function of $T_{w,0}/(-T_a)$ for various values of h_{ia}/h_{wi}. The ratio is small corresponding to small values of $T_{w,0}/-T_a$ (either large initial water temperatures or small subfreezing air temperatures) and large values of h_{ia}/h_{wi} (large wind speeds or slow flow velocities). Negative values of the ratio correspond, of course, to cases where $\phi_{wi} < \phi_{wa}$, which physically may be interpreted as those conditions for which ice will thicken because the heat loss to the atmosphere is greater than the heat delivered to the undersurface by the flow. To put the situation into better perspective, Figure 4 presents values of the ratio for particular values of $T_{w,0}$, h_{wa}, h_{wi} and T_a.

Which of the two criteria for the ice edge location is operative depends on the sequence of air temperatures. Clearly, water will not freeze until its temperature has decreased to 0°C. Thus, unless a prior ice cover is present, the most upstream location of the ice edge is given by the 0°C isotherm, corresponding to the criterion represented by eq 21. On the other hand, if an ice cover is present and the ice edge is receding downstream due to melting, it will only recede to the location at which the melting from below equals the tendency to thicken from above. Thus, during periods of warming air temperatures when the ice edge is receding downstream, the criterion of heat balance represented by eq 23 applies. During periods of cooling air temperatures, the 0°C isotherm location governs first ice appearance and eq 21 applies. In the simulation that follows, the order of logic in the calculation of ice thickening results in either the 0°C criterion or the heat balance criterion being naturally satisfied, although the latter is only approached asymptotically in time because of the unsteady nature of the calculations.

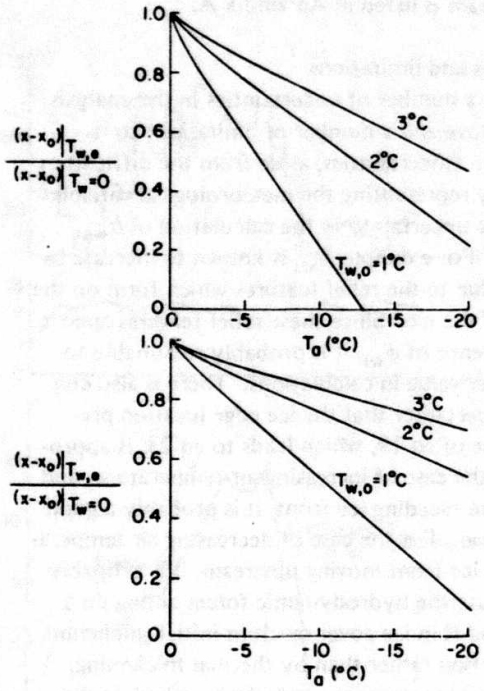

Figure 4. Comparison of distances downstream to edge of ice cover for the criteria of equilibrium heat fluxes and 0°C isotherm location as function of the air temperature and initial water temperature.

Figure 3 serves mainly to indicate the conditions for which the 0°C isotherm criterion is a poor approximation for the location of the ice edge under steady state conditions. The numerical simulation presented below is sufficiently simple computationally that the unsteady effects of T_a may also be included. The regions for which the ratio is negative, of course, are where the analysis presented herein is most useful, as the 0°C criterion would predict finite lengths of open water while, in fact, no open water will exist except in the very near field. This region also corresponds to the conditions which Silberman (1974), in a discussion of Paily et al.'s (1974) analysis, suggested resulted in plunging of the warm discharge beneath a cooler, but lighter, layer of near 0°C water. Such a plunging phenomenon undoubtedly occurs for small velocities and small densimetric Froude numbers and clearly is the case for warm water flowing into large bodies of water. Similarly, the reappearance of open water downstream from an ice-covered reach may be explained by the existence of a larger velocity downstream from a region of smaller velocity, since ϕ_{wi} is increased more or less proportionally to the velocity. The effect would be more likely to occur where the lower velocity results from increased depth rather than from increased width, since increased depth results in slower attenuation of T_w due to ϕ (through the velocity effect) than occurs by simple reduction of velocity as a result of width increase (since U has small effect on the attenuation of T_w). The above reasoning is perhaps made more clear by examination of the decrease in T_w with distance described by eq 14, which is presented in Figure 2. Again, the analysis about to be described would allow quantitative examination of specific cases.

Numerical simulation

The numerical simulation is quite straightforward. The temperature evolution along a reach is computed using eq 5 in the difference form

$$T_{w_j}^{i+1} = T_{w_j}^{i} - \frac{\phi}{\rho C_p D}\Delta t \qquad (25)$$

where the superscript i denotes a time step, and the subscript j denotes a distance node. Since eq 25 is in the Lagrangian sense, this requires that $\Delta x_j = U_j \Delta t$. This requires, in turn, that the total reach be subdivided into subreaches with lengths varying if U varies but this presents no serious problem. Typical time steps used were of the order of 1200 to 1800 seconds. At the conclusion of each time step, the thickness of the ice was determined at each j node point using eq 20 written in the form

$$\eta_j^{i+1} = \eta_j^i + \frac{1}{\rho_i \lambda}\left[\frac{T_m - T_a}{\frac{\eta_j^i}{k_i} + \frac{1}{h_{ia}}} - h_{wi}\left(T_{wj}^{i+1} - T_m\right)\right]. \qquad (26)$$

The initial temperature at the upstream end of the subreach was specified for each time as was the air temperature. For the examples presented, daily averages were used although it would be quite easy to specify a more detailed time variation. In the calculation of ϕ at each j node point, it was necessary to use either eq 6 or eq 8, depending on whether the surface was open or ice-covered. In the thickness calculations, ϕ_i was taken equal to zero if $T_a > 0$°C. After the new ice thickness was calculated, it was set equal to zero if a negative value resulted. In the example simulations presented here, h_{wa} and h_{ia} were assumed equal.

The problem also requires specifications of initial conditions. In Figure 5 are presented two examples of the effect of specifying a constant-thickness initial ice cover of either zero or finite thickness. T_a was maintained at a constant value of -5°C. The distance to ice edge stabilizes, after many days, for the finite initial thickness of 0.3 m and, after several days, for the zero initial thickness. In the latter case, the time

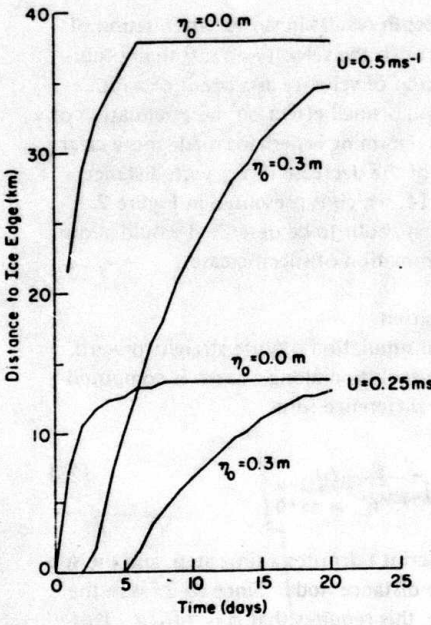

Figure 5. Example simulation of the movement of the ice edge in response to an abrupt release of thermal effluent for different assumed initial ice conditions.

to stabilize is longer than the time of travel to the equilibrium ice edge location because ice is grown until the temperature front reaches the ice edge and this ice, in turn, must be melted before equilibrium is achieved. A better set of initial conditions could probably be obtained by running the simulation for a few days prior to the period under investigation. Figure 5 also illustrates the potential errors in neglecting the energy required to melt the ice cover in the steady-state analyses referred to earlier.

There is one particular circumstance where the above analysis must be modified. When the air temperature is cooling, the ice edge location moves upstream. However, eq 26 is not applicable here until an ice cover exists and ice will not form until the water has cooled to 0°C. In this case, the 0°C isotherm location is the more correct location than the location given by the case corresponding to $\phi_{wi} = \phi_{wa}$ as $\eta \to 0$ (eq 23 in the steady-state case). There are thus two locations for the ice edge, depending on the prior history of the ice cover extent.

Finally, while no complete field data are available at the time of writing the simulation has been applied to the 1965 data presented by Dingman et al. (1967) but with an estimate of $T_{w,0}$, U and D. The results are presented in Figure 6 and show reasonable agreement with the three observations available.

The program is listed in Appendix A.

Uncertainties and limitations

There are a number of uncertainties in the analysis presented above and a number of limitations to its applicability. Uncertainties, aside from the difficulties of accurately representing the meteorological variables, include some uncertainty in the calculation of h_{wa}, h_{wi} and h_{ia}. For example, h_{wi} is known to increase by about 50% due to the relief features which form on the underside of the ice. Since these relief features appear as a consequence of ϕ_{wi}, it is probably reasonable to use the higher value in calculations. There is also considerable uncertainty that the ice edge location predicted by use of eq 19, which leads to eq 23, is appropriate. For the case of increasing air temperatures and a downstream receding ice front, it is probably a good approximation. For the case of decreasing air temperatures and an ice front moving upstream, it is probably poorer because the hydrodynamic forces acting on a newly formed thin ice cover result in initial thickening by accumulation rather than by thermal thickening. One possible improvement would be to calculate the ice production under such cases and locate the ice front by use of the equilibrium accumulation thickness predicted by the analysis of Pariset and Hausser (1961). Even that approach, however, would be limited by the fact that above a velocity of about 0.6 m s^{-1} it is difficult for a cover to even form by such accumulation.

The limitations imposed by the simplifications of the analysis are several. Longitudinal mixing has been neglected but this is considered to have a negligible effect compared with the thermal inertia of the ice cover itself. The assumption of complete vertical mixing makes the analysis inappropriate for locations very close to the source of thermal effluent, unless the effluent is already fully mixed as is the case for reservoir discharges. The assumption of complete mixing across the width of the flow, and consequent neglect of lateral mixing and dispersion, is important both near the source of the effluent and well downstream near the location of the ice front. The source problem is reasonably self-evident. At the ice front, the limitation occurs because of variations in depth and velocity across the width of the flow which, because of the resulting lateral variations in dT_w/dt, cause a laterally uniform temperature distribution to become non-uniform. Thus, it is common that the ice front is observed to be somewhat V-shaped, with the apex of the V downstream and near the thalweg of the channel. These latter effects are currently under analysis by introducing lateral mixing into the formulation and require the additional consideration that the dispersion coefficient for closed surface flow is approximately half that for open surface flow at the same depth.

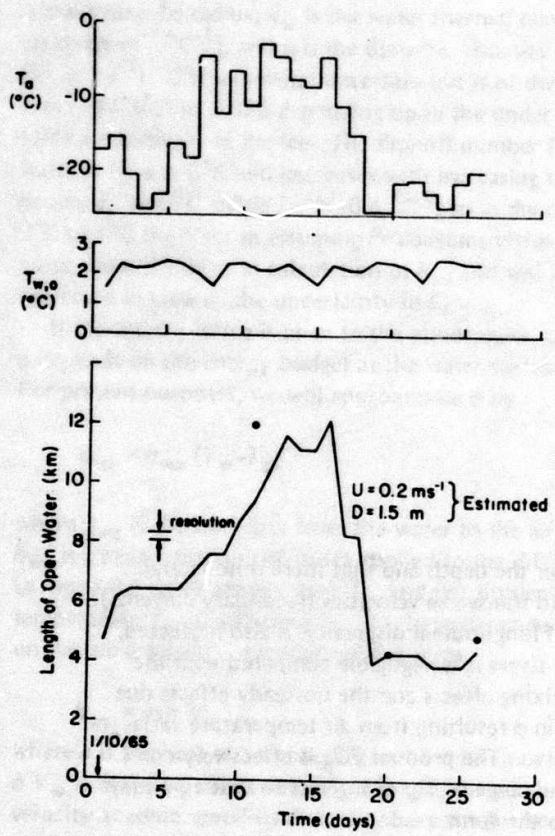

Figure 6. Comparison of simulation results to observations for Riverside location in 1965. Top figures are the air temperature and release water temperature variations. Bottom figure is the simulation result (solid line) and observations (plotted points).

Finally, the hydraulics of the flow have been assumed to be steady. This is a serious limitation but could, in principle, be overcome by frequent use of numerical models of open-channel flow to calculate the applicable velocities and depths at various stages of the simulation. These models should include the effect of ice cover on the flow but are substantially uncoupled from the thermal analysis.

LITERATURE CITED

Ashton, G.D. and J.F. Kennedy (1972) Ripples on underside of river ice covers. *J. Hydraul. Div., ASCE*, vol. 98, p. 1603-1624.

Dingman, S.L., W.F. Weeks and Y.C. Yen (1967) The effect of thermal pollution on river-ice conditions. U.S. Army Cold Regions Research and Engineering Laboratory Research Report 206. AD 666 205, AD 694 372.

Donchenko, R.V. (1978) Conditions for ice jam formation in tailwaters. CRREL Draft Translation 669.

Paily, P.P., E.O. Macagno and J.F. Kennedy (1974) Winter-regime thermal response of heated streams. *J. Hydraul. Div. ASCE*, vol. 100, p. 531-551.

Pariset, E. and R. Hausser (1961) Formation and evolution of ice covers on rivers. *Trans. Eng. Inst. Canada*, vol. 5, p. 41-49.

Rohsenow, W.M. and H.Y. Choi (1961) *Heat, mass, and momentum transfer*. Englewood Cliffs, N.J.: Prentice-Hall, Inc.

Silberman, E. (1974) Discussion of Paily, Macagno, and Kennedy, 1974. *J. Hydraul. Div. ASCE*, vol. 100, p. 1859-1860.

Weeks, W.F. and S.L. Dingman (1972) Thermal modification of river ice covers: Progress and problems. IHD/UNESCO/WMO Symp. Role of Snow and Ice in Hydrol., Banff, Alberta, vol. 2, p. 1427-1435.

PART II. EFFECT OF TRANSVERSE MIXING ON ICE SUPPRESSION

Introduction

Rivers are commonly used for the disposal of thermal wastes and, in most cases, the disposal occurs in the form of a side channel discharge of heated effluent. During periods of ice cover, the effect of such effluents is to suppress the ice cover from its otherwise natural thickening and, in the vicinity of the release, open water often results. The intent of this work is to explore the extent of this ice suppression as a function of the parameters which have most significant effect on the suppression. Part I of this report dealt with the ice suppression resulting downstream from an effluent fully mixed with the flow as would be experienced downstream from a reservoir release or from a power plant with an outfall diffuser operated so as to provide complete mixing.

Analysis of dispersion and heat loss

The governing differential equation is

$$\frac{\partial(\rho C_p T_w)}{\partial t} + U\frac{\partial(\rho C_p T_w)}{\partial x} = \frac{\partial}{\partial z}\left(E_z \frac{\partial(\rho C_p T_w)}{\partial z}\right) - \frac{\phi}{D} \qquad (1)$$

where ρ is the density (kg m^{-3}), C_p is the specific heat (J kg^{-1}°C^{-1}), T_w is the water temperature (°C), E_z is a transverse dispersion coefficient (m^2 s^{-1}), ϕ is the heat flux at the top surface (W m^{-2}), D is the depth (m), x is the longitudinal coordinate, z is the transverse coordinate, U is the mean velocity, and t is time. Equation 1 implies that mixing of the effluent with the flow is complete over the depth and that there is no lateral mixing due to transverse velocities (secondary currents). The effect of longitudinal dispersion is also neglected, although for rivers it is negligible compared with the transverse mixing effects and the unsteady effects due to variation in ϕ resulting from air temperature variations with time. The product ρC_p is effectively constant over the range of T_w of interest so that eq 1 may be written in the form

$$\frac{\partial T_w}{\partial t} + U\frac{\partial T_w}{\partial x} = \frac{\partial}{\partial z}\left(E_z \frac{\partial T_w}{\partial z}\right) - \frac{\phi}{\rho C_p D}. \qquad (2)$$

The heat flux ϕ at the surface depends on whether or not an ice cover is present. If an ice cover is present, ϕ may be reasonably represented by an expression of the form

$$\phi_{wi} = h_{wi}(T_w - T_m) \qquad (3)$$

where ϕ_{wi} is the heat flux from the water to the ice, h_{wi} is a heat transfer coefficient applied to the temperature difference $T_w - T_m$ between the flow and the ice/water surface which is at a temperature $T_m = 0$°C because of the state relation. The heat transfer coefficient h_{wi} depends on the flow variables. By analogy with closed conduit turbulent heat transfer, h_{wi} is determined from a Nusselt-Reynolds-Prandtl number correlation of the form

$$\frac{h_{wi}R}{k_w} = C\left(\frac{UR\rho}{\mu}\right)^{0.8}\left(\frac{\mu C_p}{k_w}\right)^{0.4} \qquad (4)$$

where $h_{wi}R/k_w$ is the Nusselt number, $UR\rho/\mu$ is the

Reynolds number, $\mu C_p/k_w$ is the Prandtl number, R is the hydraulic radius, k_w is the water thermal conductivity (W m^{-1} °C^{-1}), and μ is the dynamic viscosity (kg m^{-1} s^{-1}). C is somewhat uncertain but is of the order of 0.023 to 0.030 depending upon the undersurface roughness of the ice. The Prandtl number for water is 13.6 at 0°C and decreases with increasing temperature. At 0°C, $dPr/dTw \simeq -0.4$ °C^{-1}, so in the range 0°C to 4°C the error in assuming Pr constant yields at most about 5% error in calculation of h_{wi} and will be neglected in view of the uncertainty in C.

If the water surface is open to the atmosphere, then ϕ depends on the energy budget at the water surface. For present purposes, we will approximate ϕ by

$$\phi_{wa} = h_{wa} (T_w - T_a) \tag{5}$$

where ϕ_{wa} is the heat flux from the water to the air, h_{wa} is a heat transfer coefficient applied to the difference between the water temperature T_w and the ambient air temperature T_a. Coefficient h_{wa} has large dependence on the wind velocity, generally of the form

$$h_{wa} = a + b\, V_w \tag{6}$$

where a is the heat transfer coefficient for still air and $b\, V_w$ is the wind effect with V_w the ambient wind velocity at some specified distance above the surface. In numerical examples presented later, h_{wa} will be taken constant although the effect of eq 6 may easily be included in the numerical analysis (or, for that matter, h_{wa} can be calculated from even more detailed energy budget calculations of ϕ_{wa}).

The transverse mixing coefficient also depends upon whether or not the flow is ice-covered or open. We here relate E_z to a coefficient k times the product of the shear velocity U_* and hydraulic radius R in the form

$$E_z = k\, U_* R \tag{7}$$

where for open channel flow $R \simeq D$ and for covered flow $R \simeq D/2$. Denoting E_z for open flow by E_{zo} and for covered flow by E_{zi}, then

$$E_{zo} = 2E_{zi} = k\, U_* D. \tag{8}$$

Engmann (1977) has measured E_z for both covered and open flows and found results consistent with eq 8, with k in the range 0.15 to 0.2 which may be compared to a commonly used value of 0.23 (Okoye 1970). However, if the river is not straight, considerably larger values of k are observed (Paily and Sayre 1978).

The situation for a partially open ice cover where the edge of the ice cover is more or less aligned with the flow velocity is unclear. In open water areas far from the ice edge, it is reasonable to expect $E_z = E_{zo}$, while under the ice cover far from the edge $E_z = E_{zi}$. The nature of the numerical simulation presented below makes it convenient to assume an abrupt change in E_z at the ice edge. The finite difference algorithm used effectively causes a transition from E_{zo} to E_{zi} over a distance depending on the width of the grid elements.

Analysis of ice thickening and melting

The melting and thickening of the ice cover are governed by the energy balance at the water/ice interface (Fig. 1)

$$\phi_i - \phi_{wi} = \rho_i \lambda \frac{d\eta}{dt} \tag{9}$$

where ϕ_i is the heat flux by conduction through the ice cover (W m^{-2}), ρ_i is the density of ice (kg m^{-3}), λ is the heat of fusion (J kg^{-1}), η is the ice thickness (m), and $d\eta/dt$ is the rate of thickening. The conductive flux ϕ_i through the ice cover is treated in a quasi-steady manner by assuming a linear temperature profile through the ice thickness; thus,

$$\phi_i = \frac{k_i (T_m - T_s)}{\eta} \tag{10}$$

where k_i is the thermal conductivity of the ice (W m^{-1} °C^{-1}), and T_s is the top surface temperature of the ice cover and we require that $T_s \leq 0$°C because of the state relationship. In the absence of evaporation or condensation on the top surface, $\phi_i = \phi_{ia}$, where ϕ_{ia} is the heat flux from the surface to the atmosphere. ϕ_{ia} may be calculated in a manner similar to ϕ_{wa} through introduction of a heat transfer coefficient h_{ia} applied to the difference $T_s - T_a$ in the form

$$\phi_{ia} = h_{ia} (T_s - T_a). \tag{11}$$

Using $\phi_i = \phi_{ia}$ allows us to eliminate T_s between eq 10 and 11 and results in

$$\phi_i = \frac{T_m - T_a}{\frac{\eta}{k_i} + \frac{1}{h_{ia}}}. \tag{12}$$

We could also in a similar manner add the effects of a snow cover by introducing an additional term η_s/k_s in the denominator of eq 12.

Substitution of eq 12 in eq 9 then results in

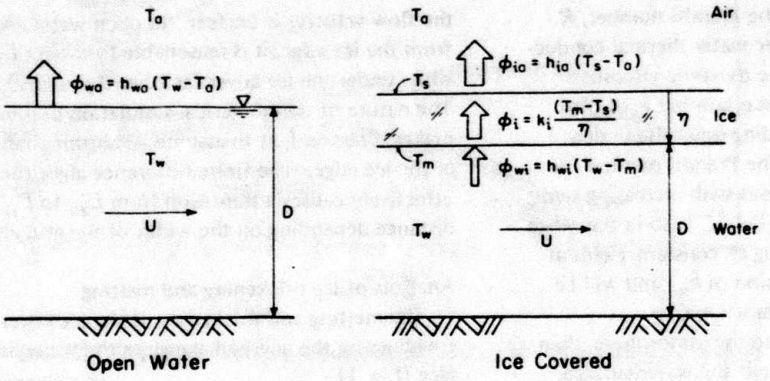

Figure 1. Definition sketch for heat transfer analysis.

$$\frac{T_m - T_a}{\frac{\eta}{k_i} + \frac{1}{h_{ia}}} - h_{wi}(T_w - T_m) = \rho_i \lambda \frac{d\eta}{dt} \tag{13}$$

which, if T_a and T_w are constant, may be readily integrated. They seldom are, however, so in the numerical analysis eq 13 will be integrated in step-wise fashion using

$$\Delta\eta = \frac{\Delta t}{\rho i \lambda}\left[\frac{T_m - T_a}{\frac{\eta}{k_i} + \frac{1}{h_{ia}}} - h_{wi}(T_w - T_m)\right] \tag{14}$$

and, of course, if the resulting value of $\eta < 0$ after a time step, then η is set equal to 0 and open water exists.

Numerical simulation

Because the numerical simulation presented below considers the effect of variations in the initial effluent temperature with time, it is convenient to transform eq 2 to a Lagrangian coordinate system moving at the mean velocity of the flow. Thus, introducing $Udt = dx$, eq 2 becomes, for a parcel of water moving with the flow,

$$\frac{DT_w}{Dt} = \frac{\partial}{\partial z}\left(E_z \frac{\partial T_w}{\partial_z}\right) - \frac{\phi}{\rho C_p D}. \tag{15}$$

The explicit finite difference equation used in the simulation is

$$\frac{T_j^{i+1} - T_j^i}{\Delta t} = \frac{(E_{j+1} + E_j)\, T_{j+1}^i - (E_{j+1} + 2E_j + E_{j-1})\, T_j^i + (E_j + E_{j-1})\, T_{j-1}^i}{2(\Delta z)^2} - \frac{\phi}{\rho C_p D} \tag{16}$$

where the E values depend on whether or not the flow is ice-covered ($E = E_{zi}$) or open ($E = E_{zo}$) at the respective j grid points. The ϕ term is also dependent on whether or not the flow is ice-covered and we choose the i, j location for the determination. Thus

$$\phi_{wi} = h_{wi}\, T_j^i \qquad \text{(ice cover present)} \tag{17}$$

$$\phi_{wa} = h_{wa}(T_j^i - T_a) \qquad \text{(open surface).} \tag{18}$$

Solving eq 16 explicitly for T_j^{i+1} results in

$$T_j^{i+1} = a\, T_{j-1}^i + b\, T_j^i + c\, T_{j+1}^i + d\, T_a \tag{19}$$

where the coefficients a, b, c and d are given by

$$a = \frac{\Delta t}{2(\Delta z)^2}(E_j + E_{j-1}) \tag{20}$$

$$b = 1 - \frac{\Delta t\, h_{wi}}{\rho C_p D} - \frac{\Delta t}{2(\Delta z)^2}(E_{j+1} + 2E_j + E_{j-1})$$

(ice cover) (21)

$$b = 1 - \frac{\Delta t\, h_{wa}}{\rho C_p D} - \frac{\Delta t}{2(\Delta z)^2}(E_{j+1} + 2E_j + E_{j-1})$$

(open surface) (22)

$$c = \frac{\Delta t}{2(\Delta z)^2}(E_{j+1} + E_j) \tag{23}$$

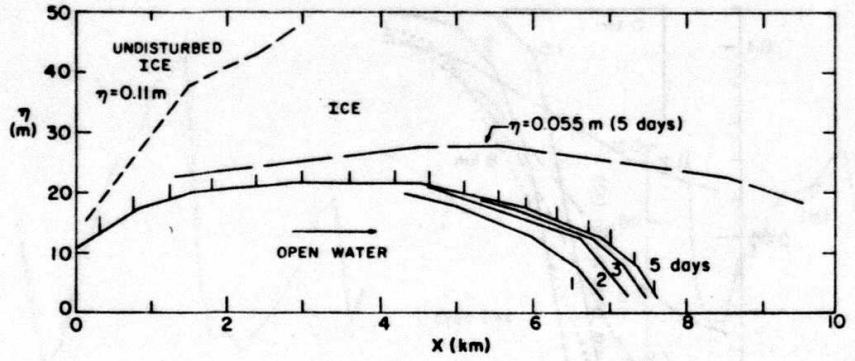

Figure 2. Results of example simulation for a smaller river under steady-state conditions.

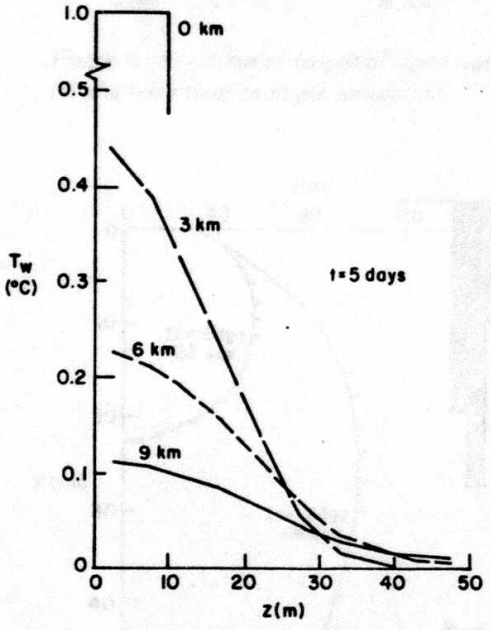

Figure 3. Lateral variation of water temperatures for example simulation after five days.

$$d = 0 \qquad \text{(ice cover)} \qquad (24)$$

$$d = \frac{\Delta t\, h_{wa}}{\rho C_p D} \qquad \text{(open surface).} \qquad (25)$$

Again, the value of the E's depends on whether or not an ice cover or an open surface is present.

The above explicit scheme is stable for

$$\frac{2E\,\Delta t}{(\Delta z)^2} < 1 \qquad (26)$$

and the appropriate value for E is, of course, E_o, since it is larger than E_i for the same total depth.

Initial conditions must also be specified. Since one seldom has detailed knowledge of ice thickness variations, the choice is practically between an initial uniform ice thickness or an initial open water condition. In either case, even for steady effluent temperatures and steady air temperatures, it takes some time for an equilibrium state to be reached. In the case of an initial zero thickness ice cover, this is due to the requirement of melting ice which has grown during the period before the thermal "front" reaches a downstream point. In the case of an initial uniform ice thickness, the time to reach equilibrium may be quite long because of the large thermal inertia of the ice cover. In the example simulations which follow the initial conditions have been taken as zero thickness and $T_w = 0°C$. In application, the most reasonable approach would seem to be to run the simulation for several days prior to the period of interest unless, of course, the situation to be investigated is the one of abrupt release of a thermal effluent.

A complete listing of the computer program may be found in Appendix B.

Example simulations

In this section two example simulations are presented. The first example is that of a smaller river 50 m wide and 2 m deep with a mean velocity of 0.5 m s^{-1}. The thermal effluent is distributed over an initial width of 10 m at a temperature of 1.0°C, which corresponds to a heat load of 42 MW. An initial thickness of 0.0 m is assumed, and the air temperature is maintained constant at -5°C. Other parameter values used are h_{wa} = 25 W $m^{-2}°C^{-1}$ (corresponding approximately to a mean wind velocity of about 4.5 m s^{-1}), $k = 0.2$, $U_* = 0.04$ m s^{-1}, and $C = 0.023$. A grid spacing of Δz = 10 m and Δx = 300 m (Δt = 600 s) was used.

In Figure 2 the ice edge location is shown for times of one, two, three, four and five days after initial thermal effluent release, and it is seen in the figure that

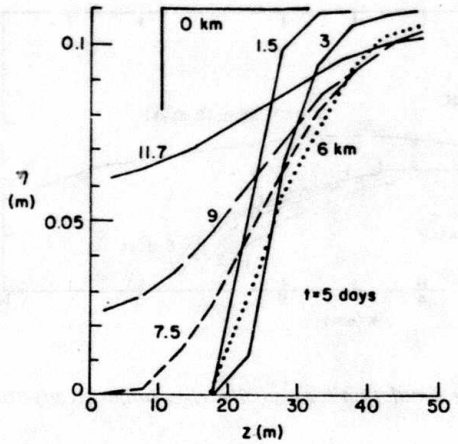

Figure 4. Lateral variation in ice thickness for example simulation after five days.

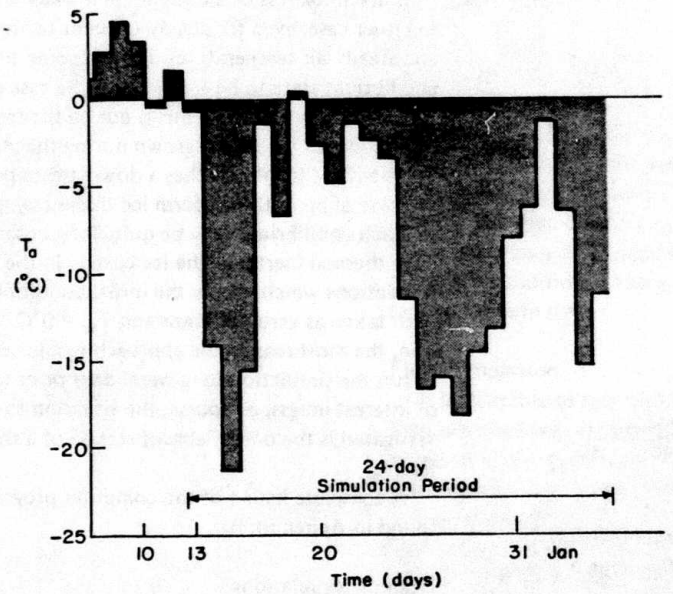

Figure 5. A typical winter daily air temperature variation used in the example simulation of a wide river.

equilibrium was achieved after about three days. Also shown in Figure 2 is the boundary of the region unaffected by the thermal effluent after five days (defined by an ice thickness differential of $\Delta\eta < 0.001$ m for $\eta = 0.11$ m) and the location at which the ice thickness was one-half its undisturbed value after five days. In Figures 3 and 4 are presented lateral profiles of water temperature T_w and ice thickness η respectively, at various distances downstream from the release point, in both cases for $t = 5$ days. We also note that had the thermal effluent been fully mixed across the width of the river at $x = 0$ the ice edge would have been located in the vicinity of 1.5 km.

The second simulation is for a very wide river, in fact sufficiently wide that reflection from the far bank has no effect on the results both because of its distance and the decrease in T_w due to heat losses to the ice cover. The flow was characterized by a depth of 4 m and a mean velocity of 0.5 m s^{-1}, and a heat load of 540 MW was distributed over an initial width of 32 m with a corresponding water temperature of 4.0°C. This heat load was maintained constant while the air tem-

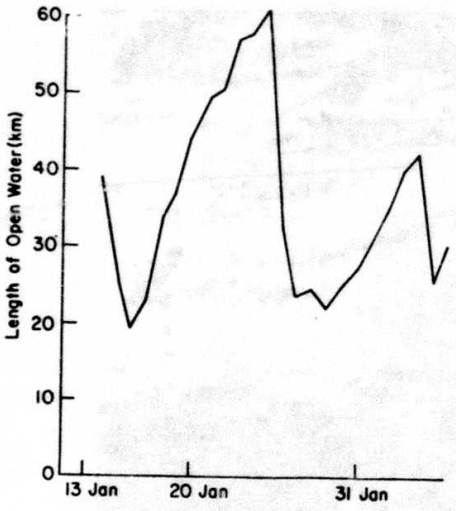

Figure 6. Variation of length of open water for the wide river example simulation.

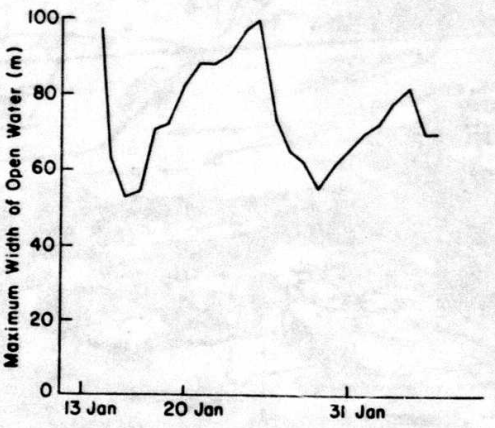

Figure 7. Variation of maximum width of open water for the wide river example simulation.

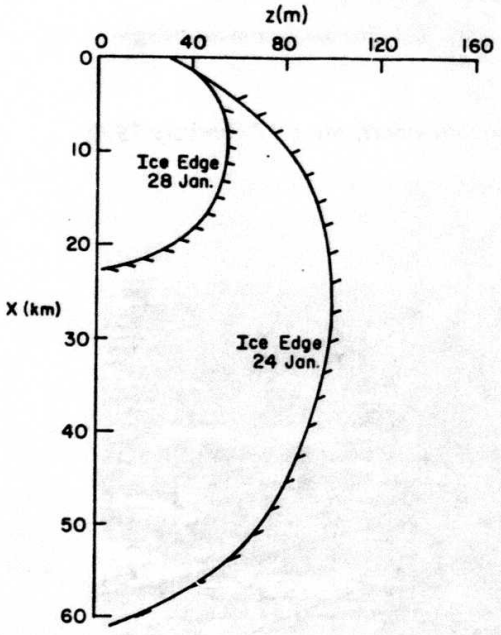

Figure 8. Maximum and minimum open water extents for the wide river example simulation.

perature varied as shown in Figure 5 (taken from an actual temperature record in the midwestern United States for 1972). An initial thickness of 0.0 m was used and other parameters were as follows: h_{wa} = 25 W m^{-2} °C^{-1}, k = 0.2, U_* = 0.04 m s^{-1}, C = 0.03, Δz = 16 m, Δx = 1350 m (corresponding to Δt = 2700 s).

Figure 6 presents the resulting length of open water and Figure 7 the maximum width of open water, the location of which varied somewhat in the longitudinal direction (from about 6 km to 25 km). The extreme cases of open water extent corresponding to 24 January (maximum extent) and 28 January (near minimum extent) are presented in Figure 8. The extreme foreshortening of the x scale relative to the z scale in Figure 8 (a ratio of 250:1) somewhat obscures how long and narrow are the open water extents. Finally we note that the example presented is also valid for a release at the centerline with a heat load of twice that used since the boundary condition at the bank ($\partial T/\partial z$ = 0) is the same by symmetry.

Field comparison

It is desirable to test the simulation against actual field observations. One very limited set of data was obtained of the open water that existed downstream of the Riverside Power Plant on the Mississippi River upstream of Bettendorf, Iowa. The data consisted of oblique angle aerial photography of the open water area and were obtained on 17 February 1979. Figure 9 shows a view of the power plant and near-field mixing zone. On the cover there is a view looking downstream from the vicinity of the plant. Figures 10 and 11 are similar views from points farther downstream. In Figure 11 an ice edge may be seen, although farther downstream there were numerous patches of open water in the plume area. Other data were obtained subsequent to the aerial photography; their sources are as follows:

River hydrography: 5 m depth fairly uniform along west side of river; obtained from hydrographic charts of the river.

Mean velocity: 0.61 m s^{-1}, obtained from a float measurement on 13 February 1979. River flow discharges were reasonably uniform over the period 13 to 17 February.

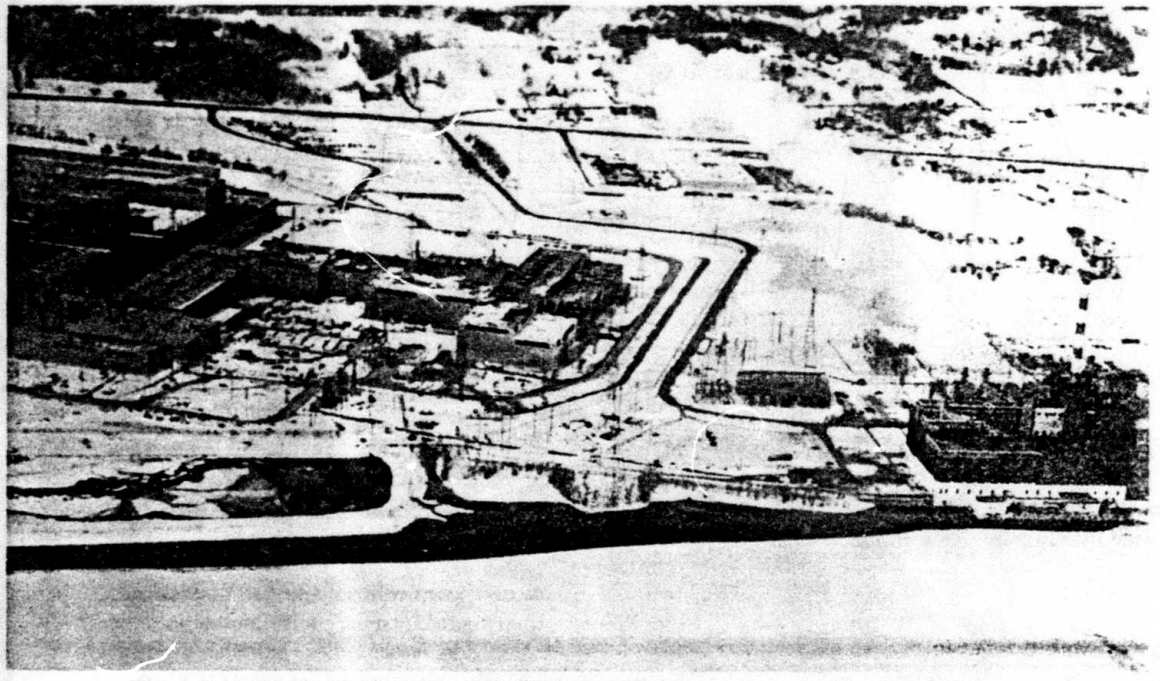

Figure 9. Power plant and near field open water of the Riverside power plant near Bettendorf, Iowa, 17 February 1979.

Figure 10. View of open water several kilometers downstream from the Riverside power plant.

Figure 11. View downstream near end of open water extent. (Our apology for the poor quality of the photograph.)

Daily air temperatures: average of daily maximum and daily minimum air temperatures recorded at the Quad-City Airport in Moline, Illinois, which is located about six miles from the river site.

Initial width of mixing: determined from aerial photography to be approximately 30 m.

Effluent source temperature: 2.97°C. This value was obtained using design temperature rise of water passing through the various plant units after correcting for plant capacity (figures supplied by Iowa-Illinois Gas and Electric Company). The effluent water was then mixed over a width of 30 m of the river flow to obtain the 2.97°C. Considerable uncertainty exists in this value since only monthly plant operating figures were available. Further, the intake and outfall geometry are sufficiently complicated that a simple near-field mixing analysis was not feasible.

Wind speed: Not recorded. In lieu of site information, h_{wa} and h_{ia} were arbitrarily taken as

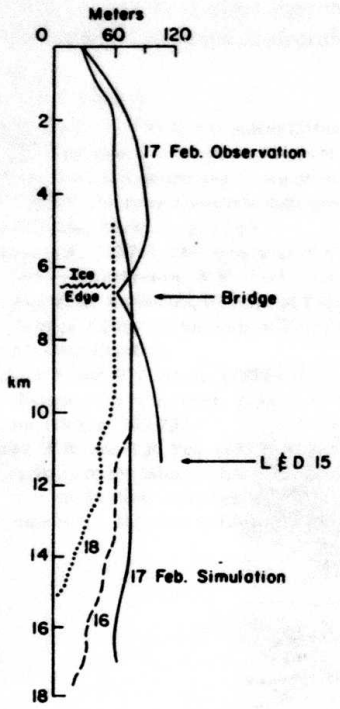

Figure 12. Comparison of numerical simulation results for 16, 17, 18 February and observed open water extent on 17 February.

25 W m^{-2} $°C^{-1}$; this corresponds approximately to an average wind speed of 4.5 m s^{-1}.

Using the above information, three simulations were run on the computer using values for the mixing coefficient of k = 0.20, 0.40 and 0.80 m^2 s^{-1}. The last value provided the best agreement with observation of the three runs and the resulting open water extent is shown in Figure 12 for the days of 16, 17 and 18 February. Also shown is the observed open water extent on 17 February.

Some interpretation of Figure 12 is in order. Approximately 7 km downstream from the plant the ice edge appears to be pinched at the location of a suspension bridge over the river. This is perhaps explained by the presence of a pier located approximately at the ice edge location which may act to stabilize the cover. At a distance of 11 km Lock and Dam 15 severely changes the local flow geometry since all the river flow passes through roller gates on the opposite side of the river. Evidence of the thermal plume existed downstream of L & D 15 but no attempts were made to simulate the complex flow conditions resulting at the dam. The simulation was arbitrarily extended using the upstream depths. The "ice edge" shown in Figure 12 is that also depicted in Figure 11. However, extensive patches of open water existed in the thermal plume area downstream and the solid line shown in Figure 12 is the outline of this area. The accuracy of the simulation is difficult to evaluate from these limited data, both because of the uncertainty in the input parameters, and because of the rapid advance upstream of the ice edge, resulting from a four-day cold period. The simulation was performed using a transverse grid interval of 15 m, a total grid width of 150 m, and a time step of 409.8 s.

It is planned to conduct a more detailed field study at this site to include direct measurement of water temperature profiles, ice extent and meteorological variables. These data will allow a better determination of the quality of performance of the simulation.

Uncertainties and limitations

The uncertainties present in the analysis largely relate to the magnitude of the coefficients used. h_{wa} and h_{ia} (assumed equal in this analysis) can always be better approximated if more extensive meteorological information is available. The magnitude of C used to estimate h_{wi} should be verified by actual field measurements and one virtue of the present work is a means of estimating whether a particular field site is sufficiently well-mixed horizontally that measurements of temperatures in the streamwise direction will accurately yield a value of C. The ice edge location results from a melting (or freezing) analysis that assumes the cover is stable for very small values of η. This is probably reasonable in the lateral direction since at the ice edge the thickness changes rapidly with z. It is less certain at the downstream edge since the ice thickness tends to "feather" and be quite thin over fairly large x distances. Other limitations in location of the downstream extent are discussed in Part I.

The analysis has assumed a uniform distribution of velocity and constant depth in the z direction which is particularly convenient since time steps then correspond to distance steps. Holley et al. (1972) have discussed the effect of lateral variations in velocity and depth on the dispersion coefficient, and it can be significant. One improvement in the present analysis would be to incorporate such effects, perhaps even with a quasi-steady shift of the velocities towards the open areas as the cover is melted away. One procedure possible is that suggested by Sayre and Yeh (1973), who utilized the Manning relationship on a local basis to determine the transverse distribution of water discharge. Finally, secondary currents can result in considerable magnification of the effective value of k when the river meanders. Incorporation of these effects would

probably require an implicit algorithm rather than the conveniently simple explicit algorithm used herein.

Literature Cited

Engmann, E.O. (1977) Turbulent diffusion in channels with a surface cover. *J. Hydraul. Res.*, vol. 15, no. 4, p. 327-335.

Holley, E.R., J. Siemons and G. Abraham (1972) Some aspects of analyzing transverse diffusion in rivers. *J. Hydraul. Res.*, vol. 10, no. 1, p. 27-57.

Okoye, J.K. (1970) Characteristics of transverse mixing in open-channel flows. W.M. Keck Laboratory of Hydraulics and Water Resources, Division of Engineering and Applied Science, California Institute of Technology, Pasadena, Report No. KH-R-23.

Paily, P.P. and W.W. Sayre (1978) Model for shore-attached thermal plumes in rivers. *J. Hydraul. Div. ASCE*, vol. 104, no. HY5, p. 709-723.

Sayre, W.W. and T.P. Yeh (1973) Transverse mixing characteristics of the Missouri River downstream from the Cooper Nuclear Station. Iowa Institute of Hydraulic Research, Report No. 145, April, 46 p.

APPENDIX A: UNSTEADY FULLY MIXED ICE SUPPRESSION

```
A *06/05/78-09:24
      C         G ASHTON 26 APRIL 1978  UNSTEADY FULLY MIXED ICE SUPPRESSION
      C         THIS PROGRAM COMPUTES DOWNSTREAM EVOLUTION OF AN ICE COVER
      C         IN RESPONSE TO RELEASE OF A FULLY MIXED THERMAL EFFLUENT
      C         AND VARYING ATR TEMP; RIVER FLOW IS ASSUMED TO BE STEADY
      C         AL,D,U,ETA, TWOUT, R  ARE LENGTH,DEPTH,MEAN VELOCITY,
      C         ICE THICKNESS,WATER TEMPERATURE, AND WIDTH FOR EACH SUBREACH
      C         DAT AND STW ARE DAILY ATR TEMPSAND EFFLUENT SOURCE TEMPS
            DIMENSION SAL(60),SR(60),SD(60),DAT(60),STW(60)
            DIMENSION AL(100),D(100),U(100),ETA(100),TWOUT(100),R(100)
            DIMENSION CHAR(70),V(70)
      C        CHAR AND V ARE DAILY HEAT TRANSFER COEF & WIND SPEED
            READ 900,NT,NSR,ALTOT,DISCH
      900   FORMAT(2I10,2F10.0)
            PRINT 816,NT,NSR,ALTOT,DISCH
      816   FORMAT(1H1,5X,'NT  NSR  ALTOT  DISCH  ',2I4,2F12.3)
      C        ALTOT IS LENGTH OF STUDY REACH (M), DISCH IS DISCHARGE (M3/S),
      C        NSR IS NUMBER OF SUBREACHES FOR WHICH VALUES OF WIDTH OF
      C        CHANNEL AND DEPTH ARE AVAILABLE
      C        NT IS NUMBER OF DAYS OF SIMULATION
            READ 901,(SR(J),SD(J),SAL(J),J=1,NSR)
      901   FORMAT (3F10.0)
            PRINT 817,(SR(J),SD(J),SAL(J),J=1,NSR)
      817   FORMAT(3X,' SR = ',F10.3,' SD = ',F10.3,' SAL = ',F10.3)
      C        SB AND SD ARE WIDTH AND DEPTH AT SUCCESSIVE X DISTANCES SAL
      C        SUBDIVIDE TOTAL REACH INTO SUBREACHES WITH DELT TRAVEL TIME
            DELT = 3600.
      C        CALCULATE NL AND TOTAL TRAVEL TIME
            TRAV = 0.0
            DO 10 J=1,NSR
      10    TRAV=TRAV+SR(J)*SD(J)*SAL(J)/DISCH
            NL=TRAV/DELT
            TRAV=TRAV/3600.
            PRINT 810,TRAV
      810   FORMAT(10X,' TOTAL TIME OF TRAVEL = ',F10.2,' HOURS')
      C        CALCULATE NEW SUBREACH LENGTHS WIT DELT TIME OF TRAVEL
            SUMSAL=SAL(1)
            SUMAL=0.0
            I=1
            DO 15 J=1,NL
            U(J)=DISCH/(SR(I)*SD(I))
            AL(J)=DELT*U(J)
            D(J)=SD(I)
            SUMAL=SUMAL+AL(J)
            DELAL=SUMAL-SUMSAL
            IF(DELAL)15,15,12
      12    I=I+1
            SUMSAL=SUMSAL+SAL(I)
      15    CONTINUE
      C        ROUTINE ONLY GOOD IF ALL SAL LONGER THAN DELT*U(J)
            PRINT 811
      811   FORMAT(3X,' AL(J)',3X,'U(J)')
            PRINT 813
      813   FORMAT(3X,' METERS',3X,'M/S')
            PRINT 812,(AL(J),U(J),J=1,NL)
      812   FORMAT(2F10.2)
      C        READ AIR TEMPERATURES AND SOURCE TEMPS FOR NT DAYS
            READ 902,(DAT(I),STW(I),V(I),I=1,NT)
      902   FORMAT(3F10.0)
            PRINT 815
      815   FORMAT(3X,' I',3X,' AIRT',3X,' WATER T)
            PRINT 814,(I,DAT(I),STW(I),I=1,NT)
      814   FORMAT(I5,2F10.4)
      C        NOW INITIALIZE PROPERTIES AND COEFFICIENTS
            CP=4215.
            AKI=2.24
```

```
      ALAM=3.34E5
      AMU=1.79E-3
      RHOI=916.
      RHOW=1000.
      CWI=1622.
      CWA=25.
C        SET ICE COVER THICKNESS AND WATER TEMPERATURE AT ZERO
      DO 25 I=1,NL
      ETA(I)=0.0
25    TWOUT(I)=0.0
      NTD=86400./DELT
      DO 30 I=1,NT
30    CWAR(I)=4.5+3.8*V(I)
50    DO 400 IT=1,NT
      CWA=CWAR(IT)
100   DO 390 IDT=1,NTD
      TWOUT(1)=STW(IT)
C      ESTABLISHES WATER TEMP FOR INLET 1ST SUBREACH
      DO 380 J=1,NL
      IF(ETA(J))250,250,300
C      NO ICE COVER
250    QW=CWA*(TWOUT(J)-DAT(IT))
      DELTW=-QW*DELT/(RHOW*CP*D(J))
      TWOUT(J)=TWOUT(J)+DELTW
C        OUTLET TEMPERATURE FOR SUBREACH AT END OF IDT TIME STEP
      IF(TWOUT(J))260,270,270
260   TWOUT(J)=0.0
      ETA(J)=DELT*CWA*(-DAT(IT))/(RHOW*ALAM)
270   GO TO 380
C      ICE COVER PRESENT
300   QW=CWI*((U(J)**0.8)/(D(J)**0.2))*TWOUT(J)
      DELTW=-QW*DELT/(RHOW*CP*D(J))
      TWOUT(J)=TWOUT(J)+DELTW
      IF(DAT(IT))306,305,305
305   QI=0.0
      GO TO 307
306   QI=-DAT(IT)/((ETA(J)/AKI)+(1./CWA))
      DETA=(DELT/(RHOI*ALAM))*(-QW+QI)
307   CONTINUE
      ETA(J)=ETA(J)+DETA
      IF(ETA(J))320,380,380
320   ETA(J)=0.0
380   CONTINUE
C     PRINT 801,(J,ETA(J),TWOUT(J),J=1,NL,20)
      DO 385 J=NL,2,-1
385   TWOUT(J)=TWOUT(J-1)
390   CONTINUE
      ALO=0.0
      DO 395 J=1,NL
      IF(ETA(J))391,391,395
391   ALO=ALO+AL(J)
395   CONTINUE
      PRINT 802,IT
      PRINT 851
851   FORMAT (3X,'ICE THICKNESSES')
      PRINT 801,(ETA(J),J=1,NL)
      PRINT 803,ALO
      PRINT 852
852   FORMAT(3X,'WATER TEMPERATURES')
      PRINT 801,(TWOUT(J),J=1,NL)
400   CONTINUE
803   FORMAT(10X,' ALO = ',F12.3,' METERS')
802   FORMAT(1H0,'END OF DAY',I5)
801   FORMAT(10F7.3)
      END
```

APPENDIX B: UNSTEADY LATERAL MIXING ICE SUPPRESSION

```
1A *05/23/78-08:06
      1.    C         G ASHTON 22 MAY 1978
      2.    C         UNSTEADY LATERAL MIXING ICE SUPPRESSION
      3.              DIMENSION AL(100),ETA(100,20),TW(100,20),DAT(60),STW(60)
      4.              READ 401,NT,NSR,NSW
      5.              READ 402,DELT
      6.              READ 403,(DAT(IT),IT=1,NT)
      7.              READ 404,(STW(IT),IT=1,NT)
      8.              READ 405,UM,DM,RW
      9.              READ 406,ATW
     10.    401      FORMAT (3I10)
     11.    402      FORMAT (F10.0)
     12.    403      FORMAT(F10.0)
     13.    404      FORMAT (F10.0)
     14.    405      FORMAT(3F10.3)
     15.    406      FORMAT(I10)
     16.    C           NOW INITIALIZE WATER TEMPERATURE AND ICE THICKNESS
     17.              DO 50 I=1,NSR
     18.              DO 40 J=1,NSW
     19.              ETA(I,J)=0.0
     20.              TW(I,J)=0.0
     21.    40        CONTINUE
     22.    50        CONTINUE
     23.    C           PRINT OUT INPUT DATA
     24.              PRINT 501,NT,NSR,NSW
     25.    501       FORMAT(3X,' NT  NSR  NSW = ',3I10)
     26.              PRINT 502,DELT
     27.    502       FORMAT(3X,' DELT = ',F12.1,' SECONDS')
     28.              PRINT 503
     29.    503       FORMAT(3X,'DAY  TA(DEG C)   TW,0')
     30.              PRINT 504,(IT,DAT(IT),STW(IT),IT=1,NT)
     31.    504       FORMAT(3X,I4,2F10.2)
     32.              PRINT 505
     33.    505       FORMAT(3X,' INITIAL ICE THICKNESSES')
     34.              PRINT 506,((ETA(I,J),J=1,NSW),I=1,3  )
     35.    506       FORMAT(20F5.3)
     36.              PRINT 507
     37.    507       FORMAT(1H0,' INITIAL WATER TEMPERATURES')
     38.              PRINT 508,((TW(I,J),J=1,NSW),I=1,3  )
     39.    508       FORMAT(20F5.2)
     40.    C           NOW ESTABLISH LENGTHS WITH TIME OF TRAVEL EQUAL TO DELT
     41.              ALSR=UM*DELT
     42.              PRINT 509,UM
     43.    509       FORMAT(1H0,3X,'MEAN VELOCITY = ',F10.3,' M PER SEC')
     44.              PRINT 510,DM
     45.    510       FORMAT(3X,'MEAN DEPTH = ',F10.3,' METERS')
     46.              PRINT 511,ALSR
     47.    511       FORMAT(3X,' SUBREACH LENGTH = ',F12.1,' METERS')
     48.              DO 60 I=1,NSR
     49.              AL(I)=ALSR
     50.    60        CONTINUE
     51.              PRINT 512,RW
     52.    512       FORMAT(3X,'TOTAL WIDTH = ',F12.1,'METERS')
     53.              DELR=RW/NSW
     54.    C           NOW DETERMINE NUMBER OF TIME STEPS PER DAY NTD
     55.              NTD=86400./DELT
     56.    C           NOW INITIALIZE PROPERTIES AND COEFFICIENTS
     57.              CP=4215.
     58.              AKI=2.24
     59.              ALAM=3.34E5
     60.              RHOI=916.
     61.              RHOW=1000.
     62.              CWI=1622.
     63.              CWA=25.
     64.              HWA=CWA
     65.              HWI=CWI*(UM**0.8)/(DM**0.2)
```

```
      F=0.05
C        F IS ARBITRARILY CHOSEN FOR EXAMPLE CASE
      USTAR=1.4*SQRT(F/8.)
      EK=0.2
C        CALCULATE STABILITY PARAMETER
C        STABLE = 2.*EK*USTAR*DX*DELT/(DELH*DELH)<1
      STABLE=2.*EK*USTAR*DX*DELT/(DELH*DELH)
      IF(STABLE-1.)70,71,71
70    PRINT 515,STABLE
515   FORMAT(3X,'STABILITY PARAMETER = ',F6.3,'  STABLE')
      GO TO 72
71    PRINT 516,STABLE
516   FORMAT(3X,'STABILITY PARAMETER = ',F6.3,' UNSTABLE')
72    CONTINUE
      PRINT 517,EK
517   FORMAT(3X,'EK = ',F6.3,' M2 PER SEC')
      PRINT 518,USTAR
518   FORMAT(3X,'USTAR = ',F7.4,' M PER SEC')
      PRINT 521,DELH
521   FORMAT(3X,'DELH = ',F7.1,'  METERS')
      EO=EK*USTAR*DX
      EI=EO/2.
      RCD=RHOW*CP*DX
      DT=DELT/(2.*DELH*DELH)
C*****************************
      DO 700 IT=1,NT
      DO 650 ID=1,NTD
C        INITIALIZE UPSTREAM WATER TEMPERATURE VARIATION
      DO 130 J=1,NTW
      TW(1,J)=STW(IT)
130   CONTINUE
      DO 650 I=NSR,2,-1
C        CALCULATE J=1 NODE
      IF(ETA(I,2))133,133,134
133   EJP1=EO
      GO TO 135
134   EJP1=EI
135   CONTINUE
      IF(ETA(I,1))136,136,137
136   EJ=EO
      B=1.-(DELT*HWA/RCD)-DT*(EJP1+   EJ)
      D=DELT*HWA/RCD
      GO TO 138
137     EJ=EI
      B=1.-DELT*HWT/RCD-DT*(EJP1+   EJ)
      D=0.
138   CONTINUE
      C=DT*(EJP1+EJ)
      TW(I,1)=B*TW(I-1,1)+C*TW(I-1,2)+D*DAT(IT)
C        CALCULATE J=NSW NODE
      IF(ETA(I,NSW-1))151,151,152
151   EJM1=EO
      GO TO 153
152   EJM1=EI
153   CONTINUE
      IF(ETA(I,NSW))154,154,155
154   EJ=EO
      B=1.-DELT*HWA/RCD-DT*(EJM1+   EJ)
      D=DELT*HWA/RCD
      GO TO 156
155   EJ=EI
      B=1.-DELT*HWI/RCD-DT*(EJM1+   EJ)
      D=0.
156   CONTINUE
      A=DT*(EJ+EJM1)
      TW(I,NSW)=A*TW(I-1,NSW-1)+B*TW(I-1,NSW)+D*DAT(IT)
C        CALCULATE INTERMEDIATE NODE POINTS
```

```
133.            DO 600 J=2,NSW-1
134.            IF(ETA(I,J-1))165,165,166
135.      165   EJM1=E0
136.            GO TO 167
137.      166   EJM1=ET
138.      167   CONTINUE
139.            IF(ETA(I,J))168,168,169
140.      168   EJ=E0
141.            GO TO 170
142.      169   EJ=ET
143.      170   CONTINUE
144.            IF(ETA(I,J+1))171,171,172
145.      171   EJP1=E0
146.            B=1.-DELT*HWA/RCD-DT*(EJP1+2.*EJ+EJM1)
147.            D=DELT*HWA/RCD
148.            GO TO 173
149.      172   EJP1=ET
150.            B=1.-DELT*HWT/RCD-DT*(EJP1+2.*EJ+EJM1)
151.            D=0.
152.      173   CONTINUE
153.            A=DT*(EJ+EJM1)
154.            C=DELT*(EJ+EJP1)
155.            TW(I,J)=A*TW(I-1,J-1)+B*TW(I-1,J)+C*TW(I-1,J+1)+D*DAT(IT)
156.      600   CONTINUE
157.      630   CONTINUE
158.      C        NOW CALCULATE ICE THICKNESSES AT J NODES
159.            DO 206 I=1,NSR
160.            DO 205 J=1,NSW
161.            IF(DAT(IT))200,200,201
162.      200   QI=-DAT(IT)/((ETA(I,J)/AKI)+1./HWA)
163.            GO TO 202
164.      201   QI=0.
165.      202   CONTINUE
166.            QW=CWT*(DM**0.8)*TW(I,J)/(DM**0.2)
167.            DELETA=(QI-QW)*DELT/(RHOI*ALAM)
168.            ETA(I,J)=ETA(I,J)+DELETA
169.            IF(ETA(I,J))203,204,204
170.      203   ETA(I,J)=0.0
171.      204   CONTINUE
172.      205   CONTINUE
173.      206   CONTINUE
174.      650   CONTINUE
175.      C        PRINT OUT DAILY RESULTS
176.            PRINT 519,IT
177.            PRINT 520,((TW(I,J),J=1,NSW),I=1,NSR)
178.      519   FORMAT (1H1,' TW DAILY END OF DAY ',I5)
179.      520   FORMAT(10X,10F6.3)
180.            PRINT 529,IT
181.            PRINT 530,((ETA(I,J),J=1,NSW),I=1,NSR)
182.      529   FORMAT(1H1,'     ICE THICKNESSES END OF DAY ',I5)
183.      530   FORMAT(10X,10F6.3)
184.      700   CONTINUE
185.            END
```

A facsimile catalog card in Library of Congress MARC format is reproduced below.

Ashton, George D.
Suppression of river ice by thermal effluents / by George D. Ashton. Hanover, N.H.; U.S. Cold Regions Research and Engineering Laboratory; Springfield, Va.: available from National Technical Information Service, 1979.
iv, 26 p., illus.; 27 cm. (CRREL Report 79-30.)
Prepared for Directorate of Civil Works - Office, Chief of Engineers by Corps of Engineers, U.S. Army Cold Regions Research and Engineering Laboratory under CWIS 31361 and 31362.
Bibliography: p. 17.
1. Cold regions. 2. Heat transfer. 3. Ice. 4. Ice openings. 5. Rivers. 6. Thermal diffusion. 7. Thermal pollution. I. United States. Army. Corps of Engineers. II. Army Cold Regions Research and Engineering Laboratory, Hanover, N.H. III. Series: CRREL Report 79-30.

☆U.S. GOVERNMENT PRINTING OFFICE: 1979 — 602-659/334